The role of the mobility law of dislocations in the plastic response of shock loaded pure metals

Gurrutxaga-Lerma, Beñat

DOI:
10.1088/0965-0393/24/6/065006

Modelling and Simulation in Materials Science and Engineering

PAPER • OPEN ACCESS

The role of the mobility law of dislocations in the plastic response of shock loaded pure metals

To cite this article: Beñat Gurrutxaga-Lerma 2016 *Modelling Simul. Mater. Sci. Eng.* **24** 065006

OPEN ACCESS
IOP Publishing
Modelling and Simulation in Materials Science and Engineering
Modelling Simul. Mater. Sci. Eng. **24** (2016) 065006 (21pp) doi:10.1088/0965-0393/24/6/065006

The role of the mobility law of dislocations in the plastic response of shock loaded pure metals

Beñat Gurrutxaga-Lerma[1]

Department of Mechanical Engineering, Imperial College London, Exhibition Rd, SW7 2AZ London, UK

E-mail: bg374@cam.ac.uk

Received 3 May 2016, revised 6 June 2016
Accepted for publication 21 June 2016
Published 11 July 2016

Abstract

This article examines the role that the choice of a dislocation mobility law has in the study of plastic relaxation at shock fronts. Five different mobility laws, two of them phenomenological fits to data, and three more based on physical models of dislocation inertia, are tested by employing dynamic discrete dislocation plasticity (D3P) simulations of a shock loaded aluminium thin foil. It is found that inertial laws invariably entail very short acceleration times for dislocations changing their kinematic state. As long as the mobility laws describe the same regime of terminal speeds, all mobility laws predict the same degree of plastic relaxation at the shock front. This is used to show that the main factor affecting plastic relaxation at the shock front is in fact the speed of dislocations.

Keywords: dislocations, plasticity, mobility law, shock loading, elastic precursor decay

(Some figures may appear in colour only in the online journal)

1. Introduction

The plastic shielding of a shock front is the fundamental process behind the attenuation of the dynamic yield point. Gurrutxaga-Lerma *et al* (2015) [1] showed that attenuation of the dynamic yield point (otherwise known as the 'elastic precursor decay') is the result the

[1] Current address: Trinity College Cambridge, CB2 1TQ, Cambridge UK.

accumulated interference of elastic waves emanating from shielding dislocations that are generated at the shock front.

This phenomenon is greatly affected by the motion of these dislocations. Dislocations are generated in shielding and anti-shielding pairs. The shielding dislocations move frontward, and as their speed approaches the transverse speed of sound, the elastodynamic fields they radiate are magnified ahead of the dislocation core in the direction of motion. The anti-shielding dislocations move in the direction opposite to the front, and as their speed approaches the transverse speed of sound, the magnitude of their elastodynamic fields behind the core in the direction of motion is weakened. This weakens the anti-shielding effect, and results in an enhanced plastic shielding of the shock front [1]. Thus, the plastic relaxation of the shock front appears to be greatly affected by the way in which dislocations move at the shock front.

In continuum elasticity descriptions of plasticity and dislocation dynamics, dislocation motion is described in terms of *mobility laws* [2]. Mobility laws express dislocation motion in their slip planes as a force or energy balance in which the action of an external stimulus (typically, an external stress) is balanced by the crystalline lattice's natural resistance to its motion (the dislocation 'drag'), and by the need to change the dislocation's own elastic self-energy.

Since dislocations move to minimise the elastic free energy of the system [3], the mobility law usually expresses the effect of the external stimuli in terms of the Peach–Koehler force [4]:

$$f_i = \epsilon_{ijk}\sigma_{lj}B_l\xi_k \tag{1}$$

where $f_i \equiv f_{\mathrm{PK}}$ is the Peach–Koehler force, ϵ_{ijk} the Levi-Civita tensor, σ_{lj} the external stress tensor, B_l the Burgers vector, and ξ_k the direction of the dislocation line.

Equally, the effect of the lattice resistance is expressed as a drag force, the nature of which depends on the speed the dislocation is moving at. At low stresses and low strain rates, dislocation motion is naturally impeded by the Peierls barrier, and the motion is governed by the thermally assisted probability of overcoming that barrier [5]. At higher stress levels, dislocations are able to overcome the barrier and enter a free glide regime where the drag force is said to resemble a viscous drag force [5], where the glide speed is reported to be proportional to the applied resolved shear stress, τ:

$$v_{\mathrm{glide}} = \frac{\tau B}{d} \tag{2}$$

where d is a drag coefficient and $B = |\mathbf{B}|$ the magnitude of the Burgers vector, both dependent on the material.

This '*free glide*' or '*pure drag*' regime and, consequently, equation (2), neglect the importance the dislocation's self-energy may have in its own motion. It is known that the latter increases with the dislocation's speed [5–7], and that according to first order linear elasticity, it diverges at the transverse speed of sound, which has led the latter to be regarded as a limiting speed of dislocations [5]. This effect results in a well-attested [5, 6, 8, 9] saturation of the speed a dislocation may achieve with respect to increasing Peach–Koehler force; due to its similarity with the relativistic motion of electric charges, this regime is often referred to as *relativistic regime*. Additional likely effects resulting from the fast moving dislocations [8, 10], suggest that the intrinsic lattice resistance may be different from the viscous drag given by equation (2), which complicates the proposal of a univocally clear mobility law valid in the relativistic regime.

This is particularly relevant for shock loading, where due to the magnitude of the applied loads, most dislocations are believed to glide in either the pure drag regime or, more usually, in the relativistic regime (see [5, 8]). Most of the proposed dislocation mobility laws that can be employed in shock loading are therefore speculative at best. Nonetheless, there seems to be

a large consensus in that the dislocation's speed should saturate as it approaches the transverse speed of sound [5, 6, 9, 11–14] or, in the presence of free surfaces, the Rayleigh wave speed [5, 15].

This article examines the role mobility laws may have in determining the plastic relaxation of a shock front propagating through FCC aluminium employing dynamic discrete dislocation plasticity (D3P). Therefore, all results presented here apply for the motion of pure edge dislocations in pure metals, thereby lacking impurities or any other such defects that may affect the dislocation's drag. In section 2, the mobility laws that will be put to test are introduced. Section 3 presents the details of the D3P simulations where the mobility laws will be tested, as well as their significance to the study of plastic relaxation in shock loading. Section 4 presents the results of this study, and offers a physical interpretation of the latter. Section 5 summarises the main findings of this work.

2. Mobility laws of high speed dislocations

The requirement that the dislocation's speed saturates as it approaches the transverse speed of sound can be satisfied in a number of ways. On one hand, one can simply fit experimental or atomistic simulations data to mathematical functions that phenomenologically describe the speed of the dislocation as τ varies; hereafter, the resulting mobility laws are called *phenomenological* mobility laws. On the other hand, one can attempt to produce physically insightful models that attempt to capture, partially at least, the physical effects that fast moving dislocations encounter; the resulting laws, here termed *inertial* mobility laws, typically involve an inertia-like force.

This section will review a number of phenomenological and inertial models that have been suggested in the past; table 1 summarises the models to be studied. This work does not intend to be an exhaustive account of all the mobility laws that have been proposed in the past. Rather, it intends to showcase the most characteristic features of those that are deemed of relevance to shock physics simulations, where dislocations are often expected to move at significant fractions of the transverse speed of sound.

2.1. Phenomenological laws

Phenomenological laws are fits to experimental or atomistic simulations data. They attempt to reproduce the observed relationship between the applied resolved shear stress, τ, and the glissile velocity of the dislocation, v, via a best fit equation. Most draw their data from experimental observations of dislocation mobility [9] or, more recently, from molecular dynamics simulations of the mobility of dislocations [22, 23]. They tend to describe only the terminal motion of dislocations, i.e. the stationary speed a dislocation reaches under the application of a constant resolved shear stress; any possible transient effect in the motion of the dislocation is generally missed.

2.1.1. Taylor's model. Gillis *et al* [16] found that the empirically observed relativistic behaviour of dislocations in many metals could be best described by modifying the linear drag coefficient in equation (2). The model, apparently originally due to JW Taylor (vid. [11]), prescribes a drag coefficient of the form

$$d = \frac{d_0}{1 - v^2/c_t^2} \tag{3}$$

where d_0 is the low speed drag coefficient and c_t the transverse speed of sound.

Table 1. Summary of the mobility laws to be studied in this work.

Type	Name	Equations	References
Phenomenological	Taylor	Equation (3)	[11, 16, 17]
Phenomenological	Power law	Equation (6)	[8, 9, 18]
Inertial	HZL	Equation (18) (with equation (16) or (17))	[19]
Inertial	Pillon *et al*	Equation (27)	[20]
Inertial	Pellegrini	Equation (29)	[21]

Gillis and Kratochvil [17] and Gilman [11] further argued that although the model neglected the acceleration time of dislocations, it was broadly valid because the acceleration times of dislocations were invariably of the order of a few picoseconds. The value of d_0 can be obtained from empirical data, and corresponds to the drag coefficient of dislocations moving in the pure drag regime, i.e. at small speeds compared to c_t.

For historical limitations, most experimental data regarding the mobility of dislocations is available only for the pure drag regime; the lack of experimental data regarding dislocations moving at speeds close to the transverse speed of sound is remedied using data obtained from molecular dynamics simulations. For instance, for FCC aluminium, experimental data suggests that $d_0 = 2 \cdot 10^{-5}$ Pa·s [5, 9]; however, experimental data for dislocations moving faster than ≈ 100 m s^{-1} in aluminium seems unavailable [8], and one must look for it in molecular dynamics simulations [22]. Nevertheless, it is found that when fitting Taylor's model to molecular dynamics data of the mobility of edge dislocations in aluminium (vid. [22]), the resulting $d_0 = 2.05 \cdot 10^{-5}$Pa·s, showing good agreement between simulations and model. This value will be employed in the following.

Employing Taylor's model, the mobility law takes the form

$$\frac{d_0}{1 - v^2/c_t^2} \cdot v = \tau B \tag{4}$$

whereby

$$v = \frac{d_0 c_t^2}{2\tau B}\left(\sqrt{1 + \frac{4\tau^2 B^2}{d_0^2 c_t^2}} - 1\right) \tag{5}$$

Equation (5) will be the one employed in the following discussion when referring to 'Taylor's model'.

2.1.2. Power law. Power law mobility laws have traditionally been favoured due to their simplicity, and because they are related to the mobility laws obtained for the regime of thermal activation of motion [18]. They take the form

$$v = v_0\left(\frac{\tau}{\tau_0}\right)^m \tag{6}$$

where m is the slope of the $\log v - \log \tau$ curve typically obtained from experimental data, and τ_0 and v_0 some reference values, the latter usually being assumed to be $v_0 = 1$. The values of m for a number of materials can be found in Nix and Menezes [9].

The problem with power laws is that they fail to capture the existence of a limiting speed to the motion of dislocations. A solution to this limitation was given by Meyers [8], who argued that each mobility regime should be given a different m exponent. Accordingly, for the pure

drag regime $m_{\text{drag}} = 1$, for the thermal activation of motion regime $m_{\text{activation}} > 1$, and for the relativistic regime $m_{\text{relativistic}} < 1$.

The material under consideration in this work is FCC aluminium. Using the MD data obtained by Olmsted *et al* [22] for FCC aluminium, one can produce a power law fit of the MD data to equation (6) where $m \approx 1$ up to $\tau = 120$ MPa with $\tau_0 = 0.035$ MPa. For values of $\tau > 120$ MPa, two additional regions are defined: one for $120 \leqslant \tau \leqslant 400$ MPa, with $m \approx 0.85$; and one for $400 \leqslant \tau \leqslant 2260$ MPa, with $m \approx 0.6$. Further increases in τ are given a value of $v = 0.98c_t = c_{\text{R}}$ (the Rayleigh wave speed), to prevent dislocations from becoming supersonic or resonating with the free surfaces [15].

2.2. Inertial mobility laws

A moving dislocation radiates energy outwards from the core in the form of elastic waves that are emitted as the dislocation moves [24]. This is reflected in changes in the dislocation's own self-energy, which is heavily dependent on the dislocation's kinematic state: as the dislocation's speed increases towards the transverse speed of sound, c_t, the elastic self-energy of the dislocation tends to increase, diverging at c_t.

The aim of inertial mobility laws is to capture theoretically the energy penalty incurred in increasing (or decreasing) the dislocation's speed in an elastic continuum. Still, unlike phenomenological laws, inertial mobility laws explicitly account for the change with speed of the elastic self-energy of the dislocation. This change is usually translated into an additional force, called the *inertia force* acting on the dislocation, the magnitude of which increases with the dislocation's speed. The dislocation's inertia force is not an inertia force in the Newtonian sense. However, as with true inertia forces, it can be shown [6, 19] that it is proportional to the dislocation's acceleration (i.e. that it opposes to changes in v, the dislocation's glide speed):

$$f_{\text{inertia}} = m\frac{\mathrm{d}v}{\mathrm{d}t} \tag{7}$$

The proportionality factor m is generally called the *mass* of the dislocation [19].

The inertia force of straight dislocation is obtained by considering the Hamiltonian (total energy) of an infinite elastic system:

$$H = T + V \tag{8}$$

where T is the kinetic energy of the dislocation, and V its elastic energy. If x is the canonical coordinate along which the dislocation glides, then Hamilton's equations require that

$$\frac{\mathrm{d}p}{\mathrm{d}t} = -\frac{\partial H}{\partial x}, \qquad \frac{\mathrm{d}x}{\mathrm{d}t} = \frac{\partial H}{\partial p} \tag{9}$$

The inertia force is then simply defined as

$$f_{\text{inertia}} = \frac{\mathrm{d}p}{\mathrm{d}t} = -\frac{\partial H}{\partial x} \tag{10}$$

If $v \equiv v_{\text{glide}}$ is the dislocation's speed, then it follows that

$$v = \frac{\mathrm{d}x}{\mathrm{d}t} = \frac{\partial H}{\partial p} = \frac{\partial H}{\partial t}\frac{\mathrm{d}t}{\mathrm{d}p} = \frac{1}{f_{\text{inertia}}}\frac{\partial H}{\partial t} = \frac{1}{f_{\text{inertia}}}\frac{\partial H}{\partial v}\frac{\partial v}{\partial t}, \tag{11}$$

whereby the dislocation's mass can be identified as

$$m = \frac{1}{v}\frac{\partial H}{\partial v}, \tag{12}$$

and the inertia force be

$$f_{\text{inertia}} = m\frac{\partial v}{\partial t} \tag{13}$$

in direct analogy with Newton's inertia.

The inertia force is a measure in changes in the self-energy of a dislocation. If the kinetic and potential energies of the dislocation are described in a linear elastic continuum, the inertia only measures changes in the energy of the system with respect to the speed of the dislocation, and therefore disregards any effect that is not taken into consideration by linear elasticity, including phonon wind and diffraction, etc, which any inertial mobility law will still have to account for, often phenomenologically. Thus, within linear elasticity inertial mobility laws will usually take the form

$$f_{\text{PK}} = m\frac{\partial v}{\partial t} + f_{\text{drag}} \tag{14}$$

where f_{drag} still needs to be obtained from elsewhere.

The key for finding f_{inertia} is therefore to find H, the system's total energy, which is not a trivial task as it needs to account for the true kinematic state of the moving dislocation. In the following, an account of some of the main proposals for an inertial mass is given.

2.2.1. Hirth–Zbib–Lothe (HZL) mass. Following the pioneering works of Frank [25], Eshelby [26] and Weertman [27], Hirth, Zbib and Lothe [19] attempted to provide a consistent definition of the mass of a dislocation, hereafter referred to as the HZL mass.

They relied on Weertman's work in deriving the elastic energy of a dislocation that has been moving with uniform speed v since $t \to -\infty$. This work reached an expression of the dislocation's energy, which for edge dislocations is of the form [28],

$$\begin{aligned} H = {} & \frac{\mu b^2}{\pi M_t^4}\ln\left(\frac{R}{r_c}\right)\left[4\sqrt{1-M_l^2}\,\frac{M_t^2}{2} - 4\frac{1-M_t^2/2}{1-M_t^2}\right. \\ & \left. + \frac{(1-M_t^2/2)^2}{2}\left(\sqrt{1-M_t^2} + \frac{6}{\sqrt{1-M_t^2}} + \frac{1}{\sqrt{1-M_t^2}^{\,3}}\right) + \frac{M_l^6}{2M_t^2\sqrt{1-M_l^2}}\right] \end{aligned} \tag{15}$$

where $M_l = v/c_l$ and $M_t = v/c_t$ are the longitudinal and transverse Mach numbers, c_l and c_t the longitudinal and transverse speeds of sound, μ the shear modulus, R and r_c the dislocation's outer and inner core width, respectively (see [5]). A similar, albeit simpler expression can be reached for screw dislocations (vid. [19, 27]). It is worth noticing that this energy is not time dependent, as it refers to a uniformly moving dislocation.

Using such elastic self-energy invariably gives rise to the paradox that a uniformly moving dislocation cannot experience an inertia force as specified by equation (13) [28, 29]. However, a mass and a pseudo-inertial force may be defined by applying equation (13) to the elastic energy given by equation (15); in that case, the inertia measures the energetic difference between two different steady states when the dislocation is in motion.

This forms the basis of the HZL mass, which provides an informed estimate of the amount the elastic self-energy of the dislocation must be increased when the latter is accelerated. Combining a Lagrangian formulation akin to the one leading to equation (11) above with the elastic energy of the uniformly moving dislocation (equation (15)), Hirth, Zbib and Lothe

[19] provided the following expressions for the mass of a dislocation, which depend on the character of the dislocation:

$$m_{\text{screw}} = \frac{\mu B^2}{4\pi} \ln\left[\frac{R}{r_0}\right] \frac{1}{v^2}\left[-\frac{1}{\gamma_t} + \frac{1}{\gamma_t^3}\right] \tag{16}$$

$$m_{\text{edge}} = \frac{\mu B^2}{4\pi} \ln\left[\frac{R}{r_0}\right] \frac{c_t^2}{v^2}\left[-8\gamma_l - \frac{20}{\gamma_l} + \frac{4}{\gamma_l^3} + 7\gamma_t + \frac{25}{\gamma_t} - \frac{11}{\gamma_t^3} + \frac{3}{\gamma_t^5}\right] \tag{17}$$

where $\gamma_l = \sqrt{1 - \frac{v^2}{c_l^2}}$, $\gamma_t = \sqrt{1 - \frac{v^2}{c_t^2}}$.

The corresponding mobility law will then be

$$B\tau = m\frac{\partial v}{\partial t} + f_{\text{drag}}(v) \tag{18}$$

where $f_{\text{drag}}(v)$ is the natural lattice resistance to the motion of dislocations (typically, $f_{\text{drag}} = d \cdot v$ from equation (2)), and m takes the forms given in equations (16) or (17) depending on whether the dislocation is of screw or edge character respectively.

2.2.2. Fully time-dependent descriptions of the inertial force. Although a good first step towards a physically motivated description of inertial effects, the HZL mass seems limited in that it relies on the kinetic energy of a dislocation that has been moving with uniform speed since $t \to -\infty$, which is an approximation for describing changes in the kinematic state of a dislocation.

Early models of fully time-dependent inertial forces. As a first step towards a more complete description of inertial force, Markenscoff and Clifton [30] employed the fully elastodynamic description of the fields of dislocation initially derived by Markenscoff [31] and Markenscoff and Clifton [7] to obtain the inertia force of an elastodynamic Volterra dislocation which jumps from rest at time $t = 0$ to a uniform speed v. They did so by calculating the energy radiated by the dislocation through a surface S_d that encloses the dislocation core:

$$\dot{H} = \int_{S_d} \left[\sigma_{ij} n_j \dot{u}_i + \left(\frac{1}{2}\sigma_{ij} u_{i,j} + \frac{1}{2}\rho \dot{u}_i \dot{u}_j\right) v\right] \mathrm{d}S \tag{19}$$

where repeated index denotes summation, σ_{ij} is the stress tensor, u_i the displacement, ρ the density, $\dot{u}_i$ the particle velocity, v the velocity of the dislocation, and $\dot{H} \equiv \frac{\partial H}{\partial t}$ for brevity.

The integral in equation (19) is a general expression of the energy release rate of a dislocation, but it seemingly depends on the choice of S_d. However, for the case of an initially quiescent dislocation that begins to move with uniform speed for $t > 0$, Markenscoff and Clifton [30] showed that the integral is independent of the choice of surface S_d (i.e. path independent), and the energy flux is uniquely determined. By making the S_d surface infinitely small about the dislocation core[2], i.e.

$$\dot{H}_0 = \lim_{S_d \to 0} \dot{H}, \tag{20}$$

[2] N.B. This case differs from that of the uniformly moving dislocation analysed by Hirth, Zbib, and Lothe in that in the latter the dislocation has been moving uniformly since $t \to -\infty$, whilst in the latter the motion starts at $t = 0$.

they were able to derive an inertial force, defined as

$$f_{\text{inertia}} = -\frac{\dot{H}_0}{v} \tag{21}$$

This expression is analogous to the one given in equation (11).

The expression for $\dot{H}_0$ depends on whether the dislocation is of screw or of edge character, and is obtained from the elastodynamic fields of uniformly moving edge and screw dislocations that were quiescent for $t < 0$ (see [7, 15, 28, 31]):

$$\dot{H}_0^{\text{screw}} = -\frac{\mu B^2}{2\pi}\frac{1}{t}\frac{1-(1-M_t^2)^{1/2}}{(1-M_t^2)^{1/2}} \tag{22}$$

$$\dot{H}_0^{\text{edge}} = -\frac{\mu B^2}{2\pi}\frac{1}{t}\left[\frac{12-8M_l^2}{M_t^2(1-M_l^2)^{1/2}} - \frac{(2-M_t^2)(6-7M_t^2)}{M_t^2(1-M_t^2)^{3/2}} - 2\left(1-\frac{M_l^2}{M_t^2}\right)\right] \tag{23}$$

The inertial expression given in equation (21) applies only for uniform motions, because for non-uniformly moving dislocations the energy release rate is strongly dependent on the past history of the dislocation [7, 32, 33] and, therefore, equation (19) will depend on the choice of S_d surrounding the core (see [29]). However, unlike the HZL inertia, the one given in equations (21)–(23) is in fact a measure of the energy radiated by a moving dislocation—the uniformly moving, elastodynamic dislocation radiates energy, unlike the stationary one employed in the definition of the HZL mass.

More recently, employing a dynamic J-integral, Ni and Markenscoff [29], found an explicit form of the inertial force for a non-uniformly moving screw dislocation. In order to avoid the singularity at the dislocation core, they introduced a regularisation of the core employing a ramp-like core and, alternatively, a mollifier. This led to an expression of both the inertia and mass of a screw dislocation of considerable complexity. No analogous expression for edge dislocations is available.

Radiative expressions of the dislocation inertia. Building on Clifton and Markenscoff's inertial force, Pillon *et al* (2007) [20] extended the inertial force to account for accelerated motion using a linear perturbative approach. Taking equation (21) as a departure point, they argued that if the dislocation's speed were a function of time, $v = v(t)$, then the differential force arising from a variation in speed δv at some time $t = \vartheta$ should be of the form

$$\delta f_{\text{inertia}} = \delta v(\vartheta)\frac{\partial f_{\text{inertia}}}{\partial v(\vartheta)} = \frac{\mu B^2}{2\pi}\delta v(\vartheta)\frac{1}{t-\vartheta}\frac{\mathrm{d}g(v)}{\mathrm{d}v} \tag{24}$$

where here the $1/(t-\vartheta) \sim 1/t$ simply accounts for a motion starting at a time ϑ other than $t = 0$, and where

$$g(v) = \frac{2\pi}{\mu B^2}\dot{H}_0\frac{t-\vartheta}{v}$$

with $\dot{H}_0$ taking either form shown in equations (22) or (23) depending on whether the dislocation is of screw or edge character, respectively.

With equation (24) in mind, the total force experienced by the dislocation can then be obtained by summing over each past contribution to $\delta f_{\text{inertia}}$:

$$f_{\text{inertia}} = \frac{\mu B^2}{2\pi} \int_{-\infty}^{t} \mathrm{d}\vartheta \frac{g'[v(\vartheta)]}{t-\vartheta} \frac{\mathrm{d}v(\vartheta)}{\mathrm{d}\vartheta}, \tag{25}$$

this has a $1/(t-\vartheta)$ singularity they regularised by replacing it with $1/((t-\vartheta)^2 + t_0^2)^{1/2}$, where t_0 is approximately the time it takes for an elastic wave to leave the core of the dislocation, to finally attain:

$$f_{\text{inertia}} = \frac{\mu B^2}{2\pi} \int_{-\infty}^{t} \mathrm{d}\vartheta \frac{\frac{\mathrm{d}v(\vartheta)}{\mathrm{d}\vartheta} g'[v(\vartheta)]}{[(t-\vartheta)^2 + t_0^2]^{1/2}} \tag{26}$$

This inertial force is then combined with a drag force to achieve the resulting mobility law:

$$\frac{\mu B^2}{2\pi} \int_{-\infty}^{t} \mathrm{d}\vartheta \frac{\mathrm{d}v(\vartheta)}{\mathrm{d}\vartheta} \frac{g'[v(\vartheta)]}{[(t-\vartheta)^2 + t_0^2]^{1/2}} + f_{\text{drag}}(v(t)) = B\tau \tag{27}$$

This defines a non-linear integral equation, which can be solved numerically via Galerkin's method. The main limitation of this equation is that it implicitly assumes that the core structure remains unchanged with speed, which is an approximation that breaks down as the dislocation's speeds approach the transverse speed of sound [29, 33].

In order to better capture observed empirical behaviour, Pillon *et al* invoked a semi-phenomenological drag force produced by Rosakis [34]:

$$f_{\text{drag}} = v(t) \cdot \frac{\eta_0 d}{\sqrt{A^2(v) + \alpha^2 \left(\frac{v}{c_t}\right)}} \tag{28}$$

where

$$A(v) = \begin{cases} \dfrac{\gamma_t}{2} & \text{for screw} \\ \dfrac{1}{2}\left(\dfrac{c_t}{v}\right)^2 \left(4\gamma_l - \dfrac{1}{\gamma_t} - 2\gamma_t - \gamma_t^3\right) & \text{for edge} \end{cases}$$

and $\eta_0 = 2m_0 c_t \frac{\alpha}{\zeta_0}$, where ζ_0 is the core width, and $m_0 = \frac{\mu B^2}{4\pi c_t^2}$. This drag force has a phenomenological component—corresponding to the linear viscous drag, d—, and a *radiative damping* component which measures the energy loss due to the elastodynamic waves emitted by the moving dislocation (i.e. the long wavelength phonons radiated by the dislocation's core); the latter can be verified to give the exact closed-form solution for steady-state motion.

A more complex mobility law, which naturally resolves the core's contractions with increasing dislocation speed as well as radiative damping, was recently proposed by Pellegrini [21, 35] employing the dynamic Peierls–Nabarro formulation previously developed by Pellegrini [33]. In this case, the inertial term accounts for all radiated wave effects by a core of varying width. The resulting inertial force is given as a complex-valued equation,

$$f_{\text{inertia}} = 2 \int_{-\infty}^{t} \mathrm{d}\vartheta \frac{m(\bar{v})}{\Delta t} \frac{\mathrm{d}\bar{v}}{\mathrm{d}\vartheta} + \frac{w_0}{c_t} \frac{\dot{\bar{\zeta}}}{\mathrm{Im}\zeta} \tag{29}$$

where $\bar{z}$ denotes the complex conjugate of z, and $\zeta = \zeta(t) \in \mathbb{C}$ is a complex position-width collective coordinate given by

$$\zeta(t) = \xi(t) + \mathrm{i}\frac{a(t)}{2} \tag{30}$$

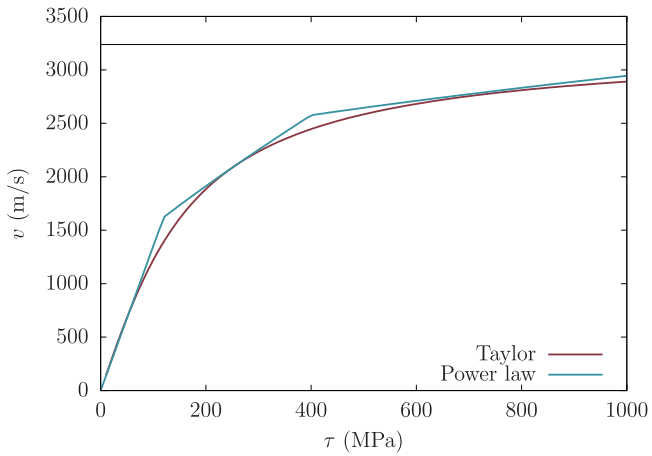

Figure 1. Phenomenological mobility laws.

with $\xi(t)$ the coordinate describing the position of the dislocation, and $a(t)$ the core width; where $\bar{v}(t)$ is a complex velocity defined as

$$\bar{v}(t,\vartheta) = \frac{\zeta(t) - \bar{\zeta}(\vartheta)}{t - \vartheta} \tag{31}$$

Pellegrini's inertial model includes the radiative, long wavelength phonon damping effect by construction, and it indeed recovers Rosakis's drag force (equation (28)) in the steady state [21]. Still, in order to account for the energy loss resulting from short wavelength phonon emission and any other damping effects, this formulation needs to invoke the viscous drag to capture the overdamped motion at low speeds. In this framework, the linear viscous drag force is written as

$$f_{\text{drag}} = \alpha \frac{w_0}{c_t} \frac{\dot{\bar{\zeta}}}{\text{Im}\zeta} \tag{32}$$

where $\alpha = 2d_0c_t/\mu$, and $w_0 = \mu B^2/(2\pi)$, and d_0 the drag coefficient.

The details to solve this equation numerically are non-trivial, and can be found in [21]. Within the limits of a linear elastic continuum, the inertial force provided by Pellegrini [21] is the most complete, physically insightful description of this effect. It must be mentioned that Rosakis' drag and Pellegrini's model allow for supersonic motion. This article shall only concern itself with subsonic dislocation motion.

2.3. Comparison between mobility laws

The two sets of mobility laws under consideration here describe the motion of a dislocation in radically different ways. Phenomenological laws only describe the *terminal speed*, i.e. the final, steady-state speed that a dislocation acquires under the action of an external applied resolved shear stress τ. Phenomenological models implicitly assume that the terminal speed is reached instantaneously (i.e. with no acceleration). Figure 1 shows the two to be employed in the following; in either case the relativistic effects are captured as a saturation of the dislocation speed with increasing τ as it approaches the limiting speed (c_t in this work). In turn, in inertial laws the terminal speed is reached only after a finite, acceleration time. The specific

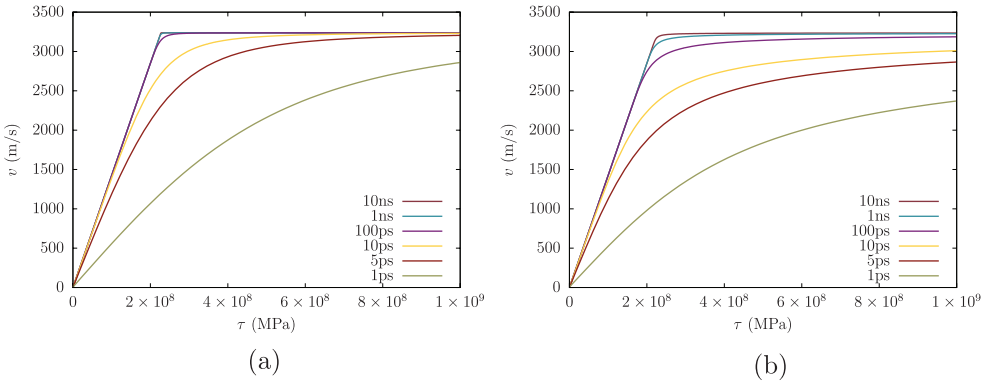

Figure 2. Mobility laws for the HZL mass. All dislocations are accelerated from rest; as can be seen, they reach terminal speeds at a relatively fast rate. (a) Solution to equation (18) for screw dislocations being accelerated from rest. (b) Solution to equation (18) for edge dislocations being accelerated from rest.

definition of the inertia force makes this time longer or shorter, and can potentially affect the dynamic behaviour of a shocked material by making fast moving dislocations more easily available to relax the structure.

In addition to the inertial force itself, all inertial mobility laws employed here require the presence of a drag force. This becomes clear at low speeds, when the inertial effects are negligible: without the drag force, the dislocation motion would be unstable [5]. Since the physical basis for the drag force (phonon emission [5, 8]) arguably remains active at higher dislocation speeds, the presence of a drag force in the mobility law seems justified. The balance between the inertial, drag and applied (Peach–Koehler) force ought to lead to a stable solution, and following an acceleration time, the dislocation ought to reach a terminal speed.

Consider for instance equation (18) from the HZL model: it ascribes all inertial effects to changes in the velocity of the dislocation. As the dislocation approaches its terminal speed, the magnitude of the inertial force decreases, and the dislocation motion will increasingly be governed by the drag force alone. When the terminal speed is reached, the inertial force vanishes, so the terminal speed can be determined as a simple balance between the Peach–Koehler force and the drag force (i.e. $f_{\text{drag}} = f_{\text{PK}}$ when $v = v_{\text{terminal}}$). This leads to two highly simplified regimes of motion for the terminal speeds of the dislocation: if the applied force is such that the speed resulting from balancing f_{drag} with f_{PK} is lower than the transverse speed of sound, c_t, then the terminal speed is determined by $f_{\text{drag}} = f_{\text{PK}}$; however, if the resulting speed is higher than c_t, the inertial force will diverge at the transverse speed of sound, and the only possible solution in equation (18) is for the speed of the dislocation plateau at c_t.

Figure 2 shows these two regimes of terminal speeds for the case of FCC aluminium ($c_t = 3237$ m s^{-1}, $c_l = 6272$ m s^{-1}, $\rho = 2700$ kg m^{-3}, $B = 2.85$ Å [1]). Following Zbib and coworkers [36–38], the drag force is chosen to be viscous and linear, with $f_{\text{drag}} = d \cdot v$, where d, the drag coefficient, is $d = 2 \cdot 10^{-5}$ Pa·s. Both the screw (figure 2(a)) and edge (figure 2(b)) cases are studied, for dislocations that are accelerated from rest under a given resolved shear stress τ. Over relatively short times the numerical solutions invariably converge to the situation described above, with a pure drag region and a region where dislocations move at the transverse speed of sound irrespective of the applied stress.

This two-regime motion seems different from the one observed both in experiments and molecular dynamics simulations of dislocation motion (vid. [8, 22]), and serves to highlight

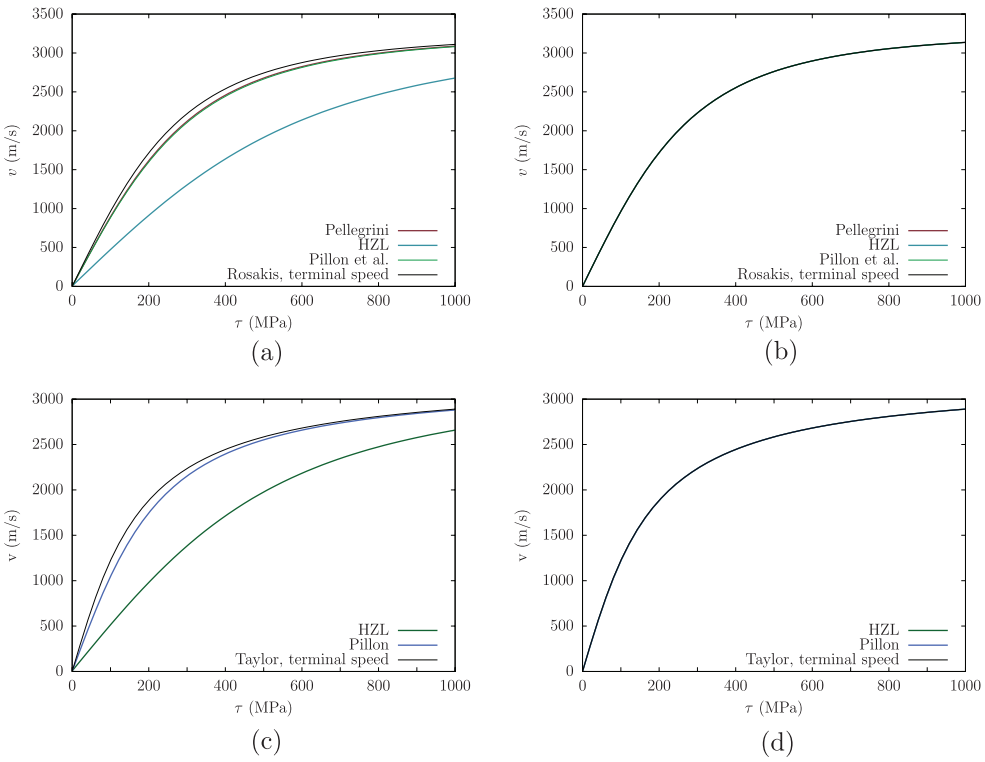

Figure 3. Comparison of the behaviour of different inertial mobility laws with Rosakis' and Taylor's drag forces. The dislocation is always an edge accelerating from rest. At 1 ps, the models of Pellegrini's [21] and Pillon *et al* [20] have almost converged to the terminal speed, whilst the HZL model is observed to be slower to reach it. Pellegrini's model is unmodified; the drag law is linear, but it recovers the Rosakis drag in the steady state. It is not combined with Taylor's drag force to avoid double counting the drag contributions. (a) 1 ps, Rosakis' drag force. (b) 10 ps, Rosakis' drag force. (c) 1 ps, Taylor's drag force. (d) 10 ps, Taylor's drag force.

that the choice of the drag force in mobility laws is crucial. In the HZL model, the inertial force dominates the acceleration times, which are therefore related to the dislocation's own self-energy. However, the terminal speed arises from the balance between the energy input (the Peach–Koehler force) and the energy dissipation within the lattice (the drag), which at high speeds is probably different from that at low speeds. Additional effects other than those causing the linear viscous drag behaviour at low speeds, such as the radiative damping discussed by Rosakis [34] and Pellegrini [21] are probably important in the relativistic regime, and should therefore be reflected in the drag force itself.

The situation in the HZL model is in a sense also reproduced by the inertial laws proposed by Pellegrini and coworkers (equations (27) and (29)): the magnitude of the inertial acceleration force tends to decrease as the dislocation approaches the terminal speed, so terminal speeds are dominated by drag effects. However, the drag force in these models is not entirely phenomenological or empirical any longer, and these models produce more informed estimates of the acceleration times.

Aside from the improved physical motivation, these two laws invariably result in shorter acceleration times compared to the HZL model's (vid. [20, 21]), so the terminal speed is reached faster; however, once the terminal speed has been reached, the behaviour of the three

models (HZL, Pillon *et al* and Pellegrini) is the same when employing Rosakis' drag force. Figures 3(a) and (b) compare the behaviour of the HZL, Pillon's and Pellegrini's models when employing the Rosakis drag force; as stated above, Pillon and Pellegrini's models tend to converge to the terminal speed faster than the HZL model, but once reached, the three models display the same behaviour.

Unlike the HZL and Pillon's model, Pellegrini's model fully accounts for radiative damping by construction, and converges to the Rosakis' drag [21], so it should not be combined with a Taylor style drag force to prevent counting the same effect twice. However, the HZL and Pillon's models can be adapted to account for relativistic drag employing Taylor's drag force rather than Rosakis'. Thus, figures 3(c) and (d) compare the behaviour of Pillon *et al*'s and the HZL model when using Taylor's drag force rather than Rosakis'. As can be seen in figures 3(c) and (d), the overall behaviour of the HZL and Pillon models is similar to that observed when using Rosakis' drag, with Pillon's model converging quicker to the terminal speeds prescribed by Rosakis's drag force (this was in fact noted by Pillon *et al* [20]). However, it must be noted that Rosakis' drag law increases faster towards the limiting speed than Taylor's; as commented in section 2.1.1; the differences are likely caused because Rosakis's drag law constrains more parameters to be physically motivated variables, rather than to fitting parameters as does Taylor's model.

Nevertheless, employing Rosakis' and Taylor's phenomenological drag force instead of the linear viscous drag leads to very similar behaviour. In both cases, all inertial models reach the terminal speed determined by the corresponding drag forces in under 10 ps: for dislocations accelerating from rest to a terminal speed in excess of $M_t = 0.8$, typical acceleration times are of the order of picoseconds. If these acceleration times are compared to those obtained for the case shown in figure 2, where the HZL model was combined with a linear drag force, a considerable difference in the acceleration times is observed; these are ascribed to the magnitude of the drag force itself, which in the case of the Rosakis or Taylor drag is considerably weaker for the same applied stress than the linear drag, so the inertia force dissipates more energy.

This highlights that the role of the inertial force is to impose an acceleration time in achieving the terminal speed; however, the terminal speed itself is governed by drag, be it phenomenologically described or via more physically insightful mobility laws such as Pellegrini's. The HZL models offers the slowest acceleration path; the acceleration times of Pillon and Pellegrini's models are shorter, and relatively similar to each other, at least for low speeds. However, in all cases the acceleration times are below $\approx$10 ps, and that applies for dislocations being accelerated from rest to speeds close to the transverse speed of sound; dislocations accelerated from a given high speed to another will invariably accelerate within shorter time scales. This result is comparable to the one found by Gillis and Kratchovil [17] for mobility laws employing the inertial mass defined by Frank [25]: the acceleration times prescribed by inertial forces are very small compared with the rise time of most shock loads. It remains to be seen what differences each of these models may entail in the plastic response of a shock loaded material.

3. A D3P study of the effect of dislocation mobility in shock loading

Dynamic discrete dislocation plasticity (D3P) was originally proposed by Gurrutxaga-Lerma *et al* [32] as the elastodynamic extension to discrete dislocation plasticity (DDP) (vid. [39]). As in DDP, dislocations are treated as Volterra discontinuities in an elastic continuum; only edge dislocations are considered, which are assumed to move under plane strain conditions along preferential slip systems, which in the plane behave like point-like particles gliding

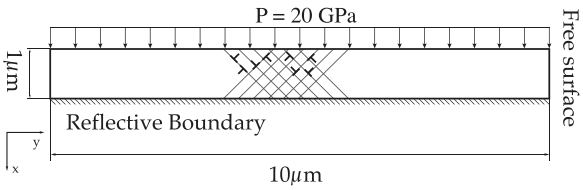

Figure 4. Schematic of the physical system to be simulated using D3P.

along preferential directions (the traces of those plane strain slip planes with the planar system). Unlike DDP however, D3P describes dislocation activity in an elastodynamic continuum, meaning that dislocation-dislocation and dislocation-medium interactions satisfy the conservation of linear momentum equation i.e. the Navier–Lamé equation for a linear elastic isotropic solid (see [40]). Time is a true field variable, and all inertial effects are accounted for [32]. As in DDP, long range interactions between dislocations are accounted for via the elastodynamic fields of dislocations; short range interactions are accounted for via constitutive laws defined in [28]. The details of D3P simulations are given in [28]. Of relevance here is that dislocations move according to the mobility laws described in table 1.

In the present study, a system of size 1 μm $\times$ 10 μm is subjected to a sudden distributed load of $P = 20$ GPa on its left side (see figure 4) with a strain rate of 10^{10} s^{-1}. The opposite right side surface is subjected to a reflective boundary condition, whilst all the rest of surfaces are left traction free. The simulated material is FCC aluminium, with Young's modulus $E = 63.2$ GPa, shear modulus $\mu = 28.3$ GPa, density $\rho = 2700$ kg m^{-3}, and Burgers vector 2.85 Å. Following [41], the plane strain slip planes for an FCC crystal are localised at $\pm 57.6°$ and 0° with respect to the shock front's direction of propagation.

As a result of the application of a sudden distributed load, a shock wave is launched propagating at the longitudinal speed of sound. The shock wave triggers dislocation activity. The sample is assumed to be initially free of any dislocations other than those forming Frank-Read sources, which in this case are treated as point-like sources (vid. [39]), and randomly distributed throughout the sample with a density of 100 sources per μm^2. Frank-Read sources are activated when a given threshold stress, the *source strength*, τ_{FR}, is overcome for a specific period of time, the *source activation time*, t_{nuc}. The source strength is inversely proportional to the length of the pinned dislocation segment l_{FR} [42], and directly proportional to the strain rate, $\dot{\epsilon}$ [43, 44]:

$$\tau_{\mathrm{FR}} = \tau_0 + \mu B \dot{\epsilon} t_{\mathrm{nuc}} \tag{33}$$

where $\tau_0 \propto 1/l_{\mathrm{FR}}$ is the quasi-static source strength, inversely proportional to the source length, which is assumed to follow a log-normal distribution [42] such that in the D3P τ_0 follows a corresponding gaussian distribution of mean 100 MPa and standard deviation 10 MPa. The nucleation time t_{nuc} is computed as described in [43], by solving the following equation:

$$\tau \cdot B = \frac{d_0}{1 - \frac{1}{c_t^2}\left(\frac{\mathrm{d}h}{\mathrm{d}t}\right)^2}\frac{\mathrm{d}h}{\mathrm{d}t} + \frac{\mu B^2}{\frac{h(t)}{2} + \frac{l_{\mathrm{FR}}^2}{8h(t)}} \tag{34}$$

which is a line tension model that tracks the outermost segment of the bowing out Frank-Read source segment via $h(t)$, it's height relative to the equilibrium unbowed position. Equation (34) is a force balance between the applied resolved shear stress, τB, that is equated to the drag force, $\frac{d_0}{1 - \frac{1}{c_t^2}\left(\frac{\mathrm{d}h}{\mathrm{d}t}\right)^2}\frac{\mathrm{d}h}{\mathrm{d}t}$, which accounts for relativistic saturation as the dislocation's

speed approaches the transverse speed of sound (see [5]), the line tension, $\frac{\mu b^2}{\frac{h(t)}{2}+\frac{l_{\mathrm{FR}}^2}{8h(t)}}$, which accounts for changes in the dislocation's elastic self-energy as the Frank-Read source segment acquires curvature. The nucleation is obtained when $h(t) = l_{\mathrm{FR}}/2$, which assumes that the Frank-Read source segment takes a semicircular shape in its unstable position; this is an *ansatz* that Gurrutxaga-Lerma *et al* [43] showed not to prejudice the accuracy of the nucleation time, which was found to be too large for Frank-Read sources to dominate the plastic response of the material at strain rates higher than $\approx 10^7\ \mathrm{s}^{-1}$.

Once activated, the Frank-Read source injects a dipole of edge dislocations, spaced a distance L_{FR} which is the minimum separation distance such that the mutual attraction between the dislocations is balanced by the applied resolved shear stress. In D3P, it is given by [43]:

$$L_{\mathrm{FR}} = \frac{-3b^4B\mu\sqrt{d^2-a^2} + 12b^2Bd^2\mu\sqrt{d^2-a^2} - }{-2a^2Bd^2\mu\sqrt{d^2-b^2} - \pi b^2 d\tau\sqrt{d^2-a^2}\sqrt{d^2-b^2} + 2Bd^4\mu\sqrt{d^2-b^2}} + \frac{-8a^2Bd^2\mu\sqrt{d^2-b^2} - 12Bd^4\mu\sqrt{d^2-a^2} + 8Bd^4\mu\sqrt{d^2-b^2}}{-2a^2Bd^2\mu\sqrt{d^2-b^2} - \pi b^2 d\tau\sqrt{d^2-a^2}\sqrt{d^2-b^2} + 2Bd^4\mu\sqrt{d^2-b^2}} \tag{35}$$

where $a = 1/c_l$, $b = 1/c_t$, $d = 1/v$ with v the dislocation speed, and τ the applied resolved shear stress.

Homogeneous nucleation follows the rules laid out in [45]. Any point along a slip plane is allowed to be a homogenous nucleation site, albeit these are spaced a distance of $10B$ to prevent newly injected dipoles from overlapping each other. Homogenous nucleation is allowed to happen if the local shear stress is greater than the lattice shear resistance, $\tau_{\mathrm{hom}} = \frac{\mu}{4\pi}$. Homogeneous nucleation is assumed to be instantaneous with respect to the simulation time step ($\Delta t = 1$ ps). Newly nucleated dislocations will be spaced following a Poisson distribution of $\lambda = 5B$ [45].

The aim of the present study is to find the different response a D3P simulation may display depending on the choice of a mobility law, following the four alternatives presented in section 2. Unless otherwise stated, the value of the model constants are those that have already been specified above.

4. Results and discussion

The data obtained from the D3P simulations is analysed by computing the stress field components due to the dislocations over sections perpendicular to the shock front. The stress profile over a given section is then averaged to reduce localisation effects, and enable easier comparison between different simulations. In this study, the principal averaging section is chosen to match the position of the elastic precursor peak, which is then tracked throughout the simulation. Thus, the results presented here correspond to the Lagrangian relaxation values over the precursor peak.

The simulation results are shown in figure 5, which compares the plastic relaxation at the precursor peak attained in the simulation of aluminium for each mobility law described in table 1. As can be seen, the degree of relaxation for each of the mobility laws tested here is remarkably similar; the main differences are found in the internal statistical variance of the results (i.e. the internal noise of the simulations), rather than in the averaged trends, which are similar enough that the differences between mobility models can be attributed primarily to the natural statistical deviations to be expected in this kind of simulations, rather than to

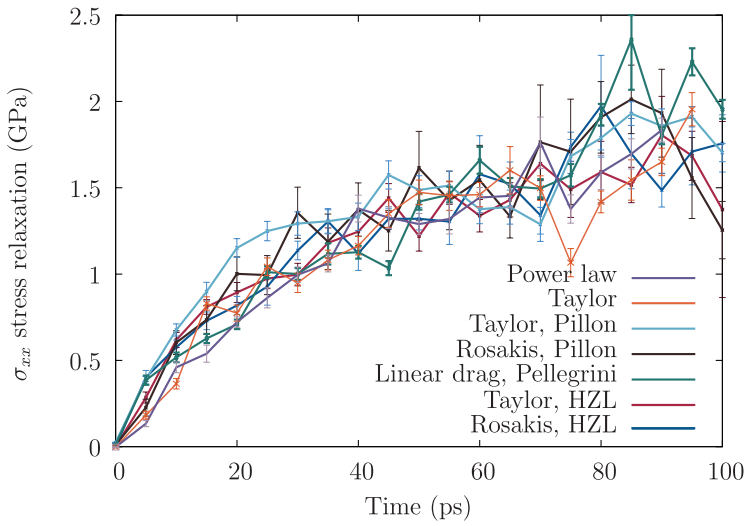

Figure 5. Comparison of the behaviour of different inertial mobility laws with Rosakis' and Taylor's drag forces. The dislocation is always an edge accelerating from rest. At 1 ps, the models of Pellegrini's [21] and Pillon *et al* [20] have almost converged to the terminal speed, whilst the HZL model is observed to be slower to reach it.

intrinsic differences in the mobility laws. The following is devoted to explore the reasons for this response.

The lack of significant variation in the results suggests that the choice of a mobility law over another might be less important than other factors affecting the simulations. In particular, the results of this work show that phenomenological laws, where acceleration times are instantaneous (i.e. where dislocations go from one terminal speed to another instantaneously) successfully track the more accurate inertial models, where acceleration times are finite albeit brief. The fact that irrespective of the acceleration times the results are broadly the same could lead one to conclude that in the shock front dislocation motion is in fact dominated, within the timescales involved, by terminal speeds, rather than by the transient motion of dislocations.

Although this is partially correct, the picture is more complex, as this effect is directly related to the way the elastic precursor decay occurs. As was shown in [1], the attenuation of the elastic precursor occurs as the result of the destructive interference of the elastodynamic waves radiated by the dislocations that are generated at the front, and that therefore act as shielding dislocations of the shock front. The magnitude of the resulting plastic attenuation is sensitive to the speed at which the relevant plastic contribution was radiated from the dislocation core. This is because as shown in [32], the Doppler-like contractions displayed by the elastodynamic fields of dislocations with increasing speed entail strong variations in the magnitude of the elastic precursor: the faster the dislocations move in the shock front, the stronger the destructive interference will be, leading to larger plastic relaxation of the shock front.

However, in the current simulations these destructive interferences are radiated at similar speeds irrespective of the chosen mobility law. This is because the simulations reported here, the dislocations at the shock front are observed to move with speeds in excess of $M_t = 0.8$ for all the mobility laws tested. Any variation in the dislocation's speed, be it an acceleration or a deceleration, is bound to make an already fast dislocation move slightly faster or slightly slower; the corresponding acceleration times (if any) are small (of the order of picoseconds), and even if the dislocation's speed varies slightly differently depending on each mobility law,

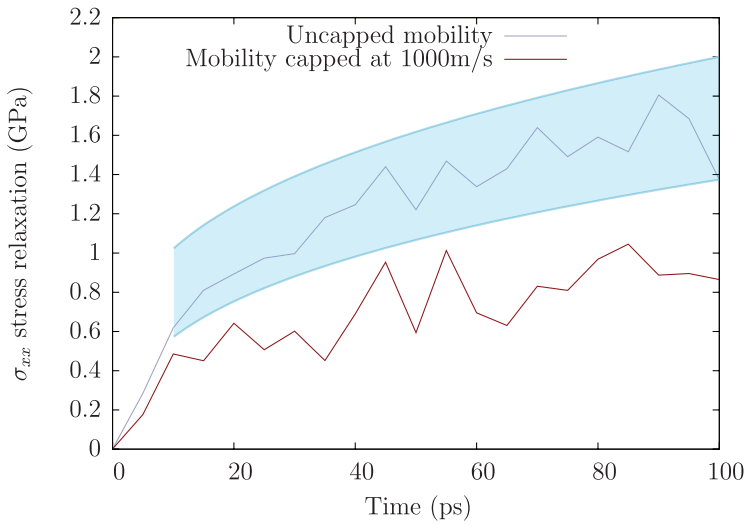

Figure 6. Degree of relaxation at the front due with different limiting speeds. The HZL model is employed as a reference.

the external applied stress is large enough that, irrespective of the mobility law chosen, this variation will be too small to lead to significant variations in the magnitude of the Doppler contractions of the dislocation's elastodynamic fields. As a result, plastic shielding remains largely unaffected.

This occurs irrespective of whether the dislocation has in fact achieved a terminal speed (as would invariably be the case for phenomenological laws) or is experiencing a transient acceleration or deceleration from one terminal speed to another (as would happen for inertial laws). In either case the dislocation will move within a range of speeds such that the resulting elastodynamic fields of the dislocations, and therefore the amount of plastic relaxation, do not see their intensity significantly affected by the nature of the current kinematic state of the dislocation.

This also suggests that the choice of a mobility law could be of relevance in situations where dislocations move at lower speeds, where finite acceleration times take place over longer timescales or widespread variations in the applied stress level occur. Such situations might be encountered in the shocked state of the material (i.e. well behind the shock front), or in the plastic shielding of dynamic cracks.

This result also shows that the attenuation of the elastic precursor is dominated mainly by fast moving dislocations at the front, since all mobility laws tested here lead to similarly fast moving dislocations for the same range of applied stresses. This could be further confirmed if the mobility laws were to provide radically different terminal speeds in the high speed 'relativistic' regime; this is not the case for the mobility laws employed in this work, as they all either quickly converge to the terminal speed, or phenomenologically match the latter. In either case the dislocations achieve speeds very close to the limiting speed in the region surrounding the elastic precursor wave's peak, so the impact these high speed dislocations have on the attenuation of the elastic precursor can be tested by artificially varying the limiting speed of the dislocations themselves. Here, this was done by capping the maximum speed dislocations might achieve to 1000 m s^{-1} (around $M_t = 0.3$). In all models the behaviour under 1000 m s^{-1} is almost linear, so a simple linear viscous drag mobility law ($\tau B = dv$), capped at 1000 m s^{-1}, was employed to simplify the D3P calculations.

Figure 6 compares the capped mobility law's results with the usual ones. As can be observed, a significant drop in the amount of plastic relaxation achieved at the front when the speed of dislocations is capped at 1000 m s^{-1}. This is a consequence of the weaker contractions that the elastodynamic fields of the shielding dislocations experience ahead of the core; these contractions would have magnified the elastodynamic relaxation of the elastic precursor, but since here the maximum speed of dislocations has been limited to a value too low for the Doppler contractions to be significant, the resulting attenuation is weaker. Further effects, such as an increased homogeneous nucleation rate at the front to compensate the weaker plastic relaxation, might play a role as the simulation advances, but it does not seem sufficient to offset the results presented here.

In the D3P simulations reported here, the capping of the terminal speed affects primarily the dislocations at the shock front itself; dislocations well behind the front are unaffected by this change in the mobility law because they move at speeds below 1000 m s^{-1}. In fact, the population of dislocations in all D3P simulations reported here is divided between fast moving dislocations at the front, which as said above reach speeds very close to the terminal speed itself; and slow moving or effectively locked dislocations behind the front, where the speeds range in between 100–500 m s^{-1}, and with a significant part of dislocations effectively stopped (i.e. with speeds lower than 100 m s^{-1}). This region of slow dislocations arises because their density is so high that they hinder each other's motion in a way similar to soft pile-ups. By virtue of causality, the relaxation at the front is produced solely by dislocations that have been generated at the front itself, so it is reasonable to argue that if the terminal speed of those dislocations is decreased, then as a result of a lessened dynamic magnification, the magnitude of the relaxation at the front will decrease as well.

In light of this, and as can be observed in the figures, the effect choosing a specific mobility law over another is found to be small, and in the simulations reported here, statistically insignificant. The main difference in the models employed here is not in the terminal speeds dislocation reach for a given applied stress, but on the acceleration path, i.e. the time it takes and the way they reach the final speed. For the phenomenological mobility laws, the acceleration time is instantaneous. For the inertial laws, the acceleration time is finite but very small[3] compared to the rise time of the shock front. Most dislocations subjected to a given stress reach their terminal speed almost instantaneously, and the role of the mobility law is limited to determining the 3 terminal speeds, which are governed by the semi-phenomenological drag forces alone.

Thus, the results presented here suggest that when studying the attenuation of an elastic precursor in a shock front, the role of inertial forces in dislocations is dual. On one hand, dislocation inertia introduces finite acceleration times, which in the previous discussion, and for the strain rate and stress levels tested, was found to be too short to impart significant differences between the response of inertial and phenomenological mobility laws; however, these effects could be of relevance for later stages of the shock front, where interlocking dislocations might lead to a regime where the applied stress varies in magnitude significantly over short periods of time. On the other hand, as done by Pellegrini [21] and Rosakis [34], dislocation inertia can be shown to explain the radiative damping contribution which, added to the viscous drag, leads to the well-known saturation of the dislocation's terminal speeds as they approach the Rayleigh wave speed (or the transverse speed of sound); phenomenological laws can only capture these effects ad hoc. In this sense, the results presented here suggest that the role of dislocation drag at high speeds, seen to dominate the plastic response of the shock front, merits further studies.

[3] Of the order of <10 ps for accelerations from rest, but generally much shorter in the D3P simulations, because dislocations transition between terminal speeds of similar magnitude, rather than experience wide changes in speed.

5. Conclusions

This article has tested the role the choice of a mobility law may have in the plastic relaxation of a shock front employing elastodynamic D3P simulations of dislocation dynamics in aluminium. Five different mobility laws have been tested: two phenomenological laws, based on data directly extracted from molecular dynamics simulations, and three inertial laws, that combine a phenomenological drag force with an inertial force measuring changes in the elastic self-energy of the dislocation as its speed varies.

The main finding of this work is that the choice of a mobility law does not significantly affect the decay of the elastic precursor, which is primarily influenced by the fastest moving dislocations. It was found that the main factor contributing to the decay is the presence of a limiting speed in the mobility law; unlike with changes of mobility law, the moment the limiting speed was reduced from the transverse speed of sound (3237 m s^{-1} in the simulations) to 1000 m s^{-1}, the decay rate diminished considerably. This highlights that the elastic precursor decay is caused by the shielding effect of fast moving dislocations, and that this shielding is all the more effective the faster the dislocations move, because the elastodynamic fields of dislocations display a Doppler contraction (magnification) ahead of themselves as they move towards the front. A decrease in the dislocation speed, as artificially imposed when capping the maximum speed to 1000 m s^{-1}, decreases this Doppler magnification.

The similarities in the result displayed by the different mobility laws are attributed to the terminal speeds each mobility law prescribes for the range of applied stress. The terminal speed is reached either instantaneously for phenomenological laws; or, for inertial laws, over a period of time too short to entail a substantial difference in the mechanical response of the shocked material. In either case, the terminal speed is determined by the drag force, which is a phenomenological component in every mobility law explored here. As a result, all models display behaviours with little statistically significant deviations. It is nonetheless likely that the finite acceleration time would become relevant for establishing the shocked state; equally, inertial laws shed light on fundamental questions such as the limiting speeds of dislocations, core effects and the possibility of supersonic dislocations. Still, the fundamental role of the drag force over the inertial force in determining the global behaviour of the shocked material highlights that experimental and atomistic observations of a saturation in the dislocation speed towards the transverse speed of sound must be attributed primarily to drag effects (be them viscous or radiative) in the motion of the dislocation through the crystalline lattice.

Acknowledgment

The author acknowledges support by the EPSRC under the EPSRC Doctoral Prize Fellowship scheme. The author is indebted to D Dini, A P Sutton and D S Balint for their comments and useful discussions. The author reports no competing interests. This work did not involve any collection of human or animal data. This work does not have any experimental data.

References

[1] Gurrutxaga-Lerma B, Balint D S, Dini D, Eakins D E and Sutton A P 2015 Attenuation of the dynamic yield point of shocked aluminum using elastodynamic simulations of dislocation dynamics *Phys. Rev. Lett.* **114** 174301

[2] Bulatov V V and Cai W 2006 *Computer Simulations of Dislocation* (Oxford: Oxford University Press)

[3] Hirth J P 1996 Dislocations *Physical Metallurgy* vol 3, ed R W Cahn and P Haasen (Amsterdam: North-Holland) ch 20, pp 1832–75
[4] Peach M and Koehler J S 1950 The forces exerted on dislocations and the stress fields produced by them *Phys. Rev.* **80** 436–9
[5] Hirth J P and Lothe J 1982 *Theory of Dislocations* 2nd edn (New York: Wiley)
[6] Weertman J 1967 Uniformly moving transonic and supersonic dislocations *J. Appl. Phys.* **38** 5293–301
[7] Markenscoff X and Clifton R J 1981 The nonuniformly moving edge dislocation *J. Mech. Phys. Solids* **29** 253–62
[8] Meyers M A 1994 *Dynamic Behavior of Materials* (New York: Wiley)
[9] Nix W D and Menezes R A 1971 Physics of strengthening mechanics in crystalline solids *Annu. Rev. Mater. Sci.* **1** 313–46
[10] Nabarro F R N 1967 *Theory of Crystal Dislocations* (Oxford: Oxford University Press)
[11] Gilman J J 1969 *Micromechanics of Flow in Solids* (New York: McGraw-Hill)
[12] Weertman J and Weertman J R 1980 Moving dislocations *Dislocations in Solids* vol 3, ed F R N Nabarro (Amsterdam: North-Holland) ch 8, pp 3–59
[13] Roos A, De Hosson J Th M and Van der Giessen E 2001 A two-dimensional computational methodology for high-speed dislocations in high strain-rate deformation *Comput. Mater. Sci.* **20** 1–18
[14] Roos A, De Hosson J Th M and Van der Giessen E 2001 High-speed dislocations in high strain-rate deformations *Comput. Mater. Sci.* **20** 19–27
[15] Gurrutxaga-Lrma B, Balint D S, Dini D and Sutton A P 2015 Elastodynamic image forces on dislocations *Proc. R. Soc.* A **471** 20150433
[16] Gillis P P, Gilman J J and Taylor J W 1969 Stress dependences of dislocation velocities *Phil. Mag.* **20** 279–89
[17] Gillis P P and Kratochvil J 1970 Dislocation acceleration *Phil. Mag.* **21** 425–32
[18] Kocks U F, Argon A S and Ashby M F 1975 *Thermodynamics and Kinetics of Slip* (*Progress in Materials Science* vol 19) (Oxford: Pergamon) ch 1, pp 1–281
[19] Hirth J P, Zbib H M and Lothe J 1998 Forces on high velocity dislocations *Modelling Simul. Mater. Sci. Eng.* **6** 165–9
[20] Pillon L, Denoual C and Pellegrini Y-P 2007 Equation of motion for dislocations with inertial effects *Phys. Rev.* B **76** 224105
[21] Pellegrini Y-P 2014 Equation of motion and subsonic-transonic transitions of rectilinear edge dislocations: a collective-variable approach *Phys. Rev.* B **90** 054120
[22] Olmsted D L, Hector L G, Curtin W A and Clifton R J 2005 Atomistic simulations of dislocation mobility in Al, Ni and Al/Mg alloys *Modelling Simul. Mater. Sci. Eng.* **13** 371–88
[23] Bitzek E and Gumbsch P 2004 Atomistic study of drag, surface and inertial effects on edge dislocations in face-centered cubic metals *Mater. Sci. Eng.* A **387–9** 11–5
[24] Markenscoff X and Ni L 2001 The transient motion of a dislocation with a ramp-like core *J. Mech. Phys. Solids* **49** 1603–19
[25] Frank F C 1949 On the equations of motion of crystal dislocations *Proc. Phys. Soc.* A **62** 131–4
[26] Eshelby J D 1949 Uniformly moving dislocations *Proc. Phys. Soc.* A **62** 307–14
[27] Weertman J 1961 High velocity dislocations *Response of Metals to High Velocity Deformation* (*Metallurgical Society Conf.* vol 9) ed P G Shewmon and V F Zackay (New York: Interscience) pp 205–49
[28] Gurrutxaga-Lerma B, Balint D S, Dini D, Eakins D E and Sutton A P 2014 *Dynamic Discrete Dislocation Plasticity* (*Advances in Applied Mechanics* vol 47) (Amsterdam: Elsevier) ch 2
[29] Ni L and Markenscoff X 2008 The self-force and effective mass of a generally accelerating dislocation I: screw dislocation *J. Mech. Phys. Solids* **56** 1348–79
[30] Clifton R J and Markenscoff X 1981 Elastic precursor decay and radiation from nonuniformly moving dislocations *J. Mech. Phys. Solids* **29** 227–51
[31] Markenscoff X 1980 The transient motion of a nonuniformly moving dislocation *J. Elast.* **10** 193–201
[32] Gurrutxaga-Lerma B, Balint D S, Dini D, Eakins D E and Sutton A P 2013 A dynamic discrete dislocation plasticity method for the simulation of plastic relaxation under shock loading *Proc. R. Soc.* A **469** 20130141
[33] Pellegrini Y-P 2010 Dynamic Peierls–Nabarro equations for elastically isotropic crystals *Phys. Rev.* B **81** 024101

[34] Rosakis P 2001 Supersonic dislocation kinetics from an augmented peierls model *Phys. Rev. Lett.* **86** 95–8
[35] Pellegrini Y-P 2012 Screw and edge dislocations with time-dependent core width: from dynamical core equations to an equation of motion *J. Mech. Phys. Solids* **60** 227–49
[36] Shehadeh M A, Bringa E M, Zbib H M, McNaney J M and Remington B A 2006 Simulation of shock-induced plasticity including homogeneous and heterogenous dislocation nucleations *Appl. Phys. Lett.* **89** 171818
[37] Shehadeh M A, Zbib H M and de la Rubia Diaz T 2005 Multiscale dislocation dynamics simulations of shock compression in copper single crystal *Int. J. Plast.* **21** 2369–90
[38] Zbib H M and de la Rubia Diaz T 2002 A multiscale model of plasticity *Int. J. Plast.* **18** 1133–63
[39] Van der Giessen E and Needleman A 1995 Discrete dislocation plasticity: a simple planar model *Modelling Simul. Mater. Sci. Eng.* **3** 689–735
[40] Achenbach J D 1973 *Wave Propagation in Elastic Solids* (*Applied Mathematics and Mechanics* vol 16) (Oxford: North-Holland)
[41] Rice J R 1987 Tensile crack tip fields in elastic-ideally plastic crystals *Mech. Mater.* **6** 317–35
[42] Shishvan S S and Van der Giessen E 2010 Distribution of dislocation source length and the size dependent yield strength in freestanding thin films *J. Mech. Phys. Solids* **58** 678–85
[43] Gurrutxaga-Lerma B, Balint D S, Dini D and Sutton A P 2015 The mechanisms governing the activation of dislocation sources in aluminum at different strain rates *J. Mech. Phys. Solids* **84** 273–92
[44] Agnihotri P K and Van der Giessen E 2015 On the rate sensitivity in discrete dislocation plasticity *Mech. Mater.* **90** 37–46
[45] Gurrutxaga-Lerma B, Balint D S, Dini D, Eakins D E and Sutton A P 2015 The role of homogeneous nucleation in planar dynamic discrete dislocation plasticity *J. Appl. Mech.* **82** 071008